Chapter 12

FLIMM and FLAMM Methods: Localization of 3-D Space Charges at the Micrometer Scale

12.1. Introduction

Polymer materials are widely used as basic insulator structures in many devices in electrical engineering, such as high voltage cables, transformers or capacitors. They have to resist strong voltage gradients, sometimes up to a few tens of kV/mm. Furthermore, engineers have to take into account important internal and local electric fields due to the presence of space charges which are trapped within the materials. These mainly result from the dissociation of electrically neutral species, charge injections at the surface of the insulator, or due to the orientation of the electric dipole.

In these zones affected by a strong local electric field, dissipative energy phenomena can lead to a premature ageing of the material, and potentially to a faster than expected breakdown of the dielectric. For these reasons, many efforts have been implemented over the past ten years in order to make more reliable the detection and characterization of these charges.

Several space charge measurement techniques have been developed [TAK 99], mostly non-destructive thermal ones. However, these methods present a very poor spatial resolution.

Chapter written by Anca PETRE, Didier MARTY-DESSUS, Laurent BERQUEZ and Jean-Luc FRANCESCHI.

With an aim to increase this resolution, we proposed to develop a technique based on the use of focused thermal excitation as a source, allowing the characterization of space charge profiles at the scale of a few tens of micrometers.

For this purpose, two investigation methods were developed: FLAMM (*Focused Laser Acoustic Modulation Method*) which detects thermo-acoustic waves generated by a laser beam using a piezoelectric sensor stuck on the rear side of the object under study, and FLIMM (*Focused Laser-Intensity Modulation Method*), an evolution of the well-known LIMM technique. In this last case, the interactions between temperature variations induced by the laser beam and the electric charges trapped in the material produce, under specific conditions, an informative signal to be processed. The main specificity of both methods lies in their ability to detect quasi-localized charges. This, combined with the scan of a given area of the sample, results in multidimensional charge cartographies that may be carried out at the micrometer scale.

12.2. The FLIMM method

12.2.1. *Principle*

The FLIMM consists of irradiating the surface of a sample using an intensity-modulated laser diode (45 mW, 658 nm) at a given frequency. This beam is focused at the surface of the sample to create a non-uniform thermal gradient inside the structure (Figure 12.1). The interaction between this thermal wave and the space charge and/or the spatial polarization produces a pyroelectric current.

The pyroelectric current is converted into voltage by a low-noise transconductance preamplifier. Then, the signal is extracted from noise by a lock-in amplifier which gives both the real and the imaginary parts of the pyroelectric current for a given modulation frequency of the beam. A mathematical treatment is then used to calculate the space charge profile. All the system is managed by a computer: laser beam frequency modulation, position of the spot beam at the sample surface, acquisition and treatment of the information signal.

From each position of the beam a current is recorded, and after the mathematical deconvolution, a 2-D representation of the in-depth space charge profile can be made. By scanning the surface with the laser, 3-D representations and cartographies of the trapped space charges are possible.

Samples are metallized on both sides with a thin gold or aluminum layer (20 to 50 nm) and placed in a measurement cell, used at the same time as a sample support and as protection against electromagnetic perturbations.

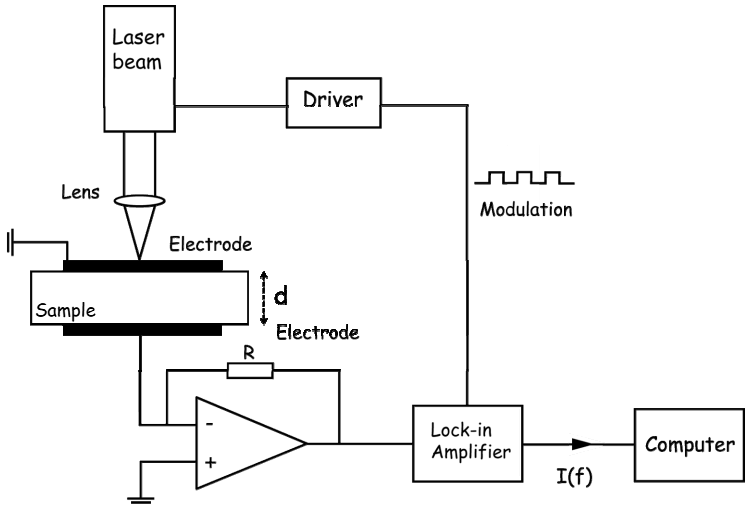

Figure 12.1. *Outline of the FLIMM set-up*

12.2.2. *Characteristic FLIMM equation*

The pyroelectric current I depends on the modulation frequency f of the laser beam, the local value of the temperature $T(z,f)$ in the sample as well as the charge function $r(z)$ (space charge $\rho(z)$ and polarization $p(z)$), z being the direction of the sample thickness at a given position of the laser beam impact.

The expression of the pyroelectric current is:

$$I(f) = j.2\pi.f.\frac{A}{L}\int_0^L r(z)T(z,f)dz$$

$$\text{with } r(z) = p(z) - (\alpha_x - \alpha_e).\varepsilon.\varepsilon_0.E(z) \qquad [12.1]$$

where $A\,(m^2)$ represents the thermal spot size, $r(z)\,(Cm^{-3})$ the total space charge, $p(z)\,(Cm^{-3}K^{-1})$ the pyroelectric coefficient, $E(z)\,(Vm^{-1})$ the internal electric field, α_x, α_ε (K^{-1}) respectively the relative dependencies of the local expansions and the electric permittivity with temperature in the material.

12.3. The FLAMM method

This method is similar to the FLIMM with regard to thermal excitation by a focused laser beam. Instead of directly recording the FLIMM current from an electrode on the sample, the electric charge Q which appears on the electrode through a piezo-electric polymer sensor (PVDF) is measured [FRA 97], [FRA 00], [HAS 97]. This plays the role of insulating capacity when the sample is subjected to a potential difference (Figure 12.2).

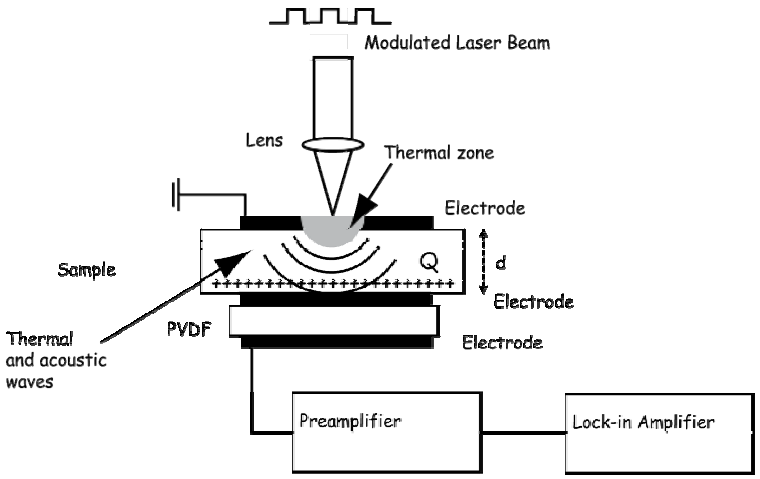

Figure 12.2. *Outline of the FLAMM set-up*

For energies and frequencies used, the contribution of thermal phenomena to the total signal is widely preponderant, compared to acoustic pressure waves phenomena induced effects. The PVDF sensor thus allows the induced charge $Q(f)$ to be measured by capacitive effect, but also records an acoustic component. This is why this technique was named FLAMM (*Focused Laser Acoustic Modulation Method*). Using uni-dimensional modeling of the temperature, the expression of the charge $Q(f)$ was established by Mopsik [MOP 82]. From this, the expression of the potential $V(f)$ measured between the electrodes of the PVDF sensor can then be deduced:

$$V(f)=\frac{\alpha_x-\alpha_\varepsilon}{\varepsilon}\int_0^L \rho(x).g(x,f)dx \text{ avec } g(x,f)=\int_0^x T(u,f)du-\frac{x}{L}\int_0^L T(u,f)du \qquad [12.2]$$

where ε represents the dielectric constant of the material, $\alpha_x, \alpha_\varepsilon\ (K^{-1})$ are respectively the relative dependencies of the local expansions and the electric permittivity with temperature in the material, and $\rho(z)\ (Cm^{-3})$ the space charge.

12.4. Modeling of the thermal gradient

In FLIMM instrumentation, it is impossible to get an evaluation of the temperature variations inside the material in an experimental way. Some methods allow the measurement of the temperature at the sample surface (bolometric set-ups for example), but none of them can give relevant information about the local temperature distribution in a volume.

The necessity to develop a coherent mathematical model to study the local internal temperature variations was then obvious. The theoretical determination of the temperature field within an insulator under irradiation is of very great importance; the accuracy of the results will depend on it. Indeed, the extraction of the charge from the Fredholm equation [12.1] requires tricky mathematical processing, and the temperature plays a primary role. Thus, several uni-dimensional and tri-dimensional models were developed. First, a uni-dimensional model was proposed, assuming a surfacic contribution of energy, which allowed a global estimation of the charge. Taking into account that the laser diode is focused on the sample surface, this model is no longer appropriate. A new model with a "four layer" volumic contribution was then developed. The particularity of this model lies in the fact that it takes into account different media constituting the sample. Indeed, heat propagation depends on the thermal characteristics of each medium and it should be considered in order to model the physical phenomenon as finely as possible.

12.5. Mathematical deconvolution

The measurement of the pyroelectric current $I(f)$ and the modeling of the temperature distribution $T(z, f)$ lead to the determination of the charge or polarization profile by using a mathematical processing of equation [12.1].

This equation is a Fredholm integral of the first kind, in which $r(x)$ is the unknown function to evaluate. Generally, equations based on such kind of integrals are very badly conditioned (with ill-posed problems), generally due to the extreme sensitivity of the system they describe. They can therefore produce an infinite set of solutions by considering the experimental error domain.

To solve this kind of equation, several mathematical deconvolution methods have been developed, from the simplest to more complex ones.

12.5.1. *Virtual Space Charge Model*

The Virtual Space Charge Model (VSCM), a simple and original model [FRA 01], allows the average space charge in a sample to be determined. The principle of this method consists of choosing a charge distribution model which would give the same signals as those detected experimentally, induced by a real charge. This means a mathematical inversion can be avoided, by exclusively relying on a comparison between the measured induced effects and those simulated by the model.

Let us consider two constant charge distributions, ρ_1 and ρ_2, representative of each half of the sample, their sum being the average charge distribution in the sample. By giving constant values to these two distributions and knowing the thermal gradient which is propagated within the material, the associated pyroelectric current can be rebuilt. This current presents a maximum I_m at a frequency f_m, independent of the material thickness.

A general variation law can be determined: $I_m = \alpha\rho_1 + \beta\rho_2$ where α and β are constants which depend on the physical properties of the material. Consequently, the maximum current can be considered as representative of the average charge in the sample.

Nevertheless, this simple and fast model is not efficient enough for the localization of charges in the material. For this purpose, other inversion methods were implemented.

12.5.2. *The scale transformation method*

The scale transformation method, based on a simplification of the temperature equation for the highest modulation frequencies used, does not require any matrix inversion. It then lead to a simplification of the pyroelectric current equation [12.1] and an approximation of the charge function $p_a(z_r)$ in the material at thickness z_r such that [PLO 92]:

$$p_a(z_r) = \frac{kL}{D\eta j_0 S}(\Re - \Im)I(\omega = 2D/z_r^2) \qquad [12.3]$$

where $\Re$ and $\Im$ are the real and imaginary parts of the pyroelectric current, D the thermal diffusivity and $z_r = \sqrt{\frac{D}{\pi f}}$.

It was shown [PLO 92] that the spatial resolution decreases with the thermal gradient penetration thickness. A good approximation is then obtained with a maximal resolution near the surface of the sample. It is therefore necessary to proceed to a second measurement on the opposite side of the material in order to obtain a complete and more reliable reconstitution of the charge profile. The main advantage of this method is that it avoids mathematical treatment likely to be hidden by the noise of experimental errors. Its development is easy and immediate.

12.5.3. *The regularization method*

A more complex but more efficient method called regularization was also developed. It consists of imposing an additional constraint on the equation system to force a unique solution [PET 04a].

The fundamental Fredholm equation, taking into account a noisy environment, is given by:

$$\int_0^1 A(s,t)x(t)dt = b_0(s) + e(s) \qquad [12.4]$$

where $b_0(s) + e(s)$ is the total measured signal, $e(s)$ the noise, $A(s,t)$ the core function and $x(t)$ the solution sought.

Since the measured signal is constituted by a finite set of values s, the continuous model [12.4] can be replaced by a discrete linear equation, such as:

$$Ax = b_0 + e = b \qquad [12.5]$$

It is not easy to solve these discrete linear equations because of the great number of small singular values which tend to increase the influence of errors. A significant solution can be calculated by using the regularization methods. Their goal consists of introducing some additional information with respect to the solution sought in order to stabilize the inverse problem, then to extract a solution expected to be close to the reality. Several additional constraints can be added, but generally a minimization of the norm (order 2) of the solution is imposed.

Different regularization methods were described by Hansen [HAN 96], [HAN 94]. Our attention was focused on the Tikhonov techniques, like *Truncated Singular Value Decomposition* (TSVD) and *Piecewise Polynomial* TSVD [TIK 77]. The difference between these two lies in the way that the additional constraints are imposed to the solution in order to reduce the influence of errors.

The most famous regularization technique was developed by Tikhonov and applied in various areas, for example in image processing [AND 77] or biomedical technology [SKI 02].

The principle of this method is based on the choice of a solution x_λ which satisfies the problem:

$$\min_x \left\{ \|Ax - b\|_2^2 + \lambda \|Px\|_2^2 \right\} \qquad [12.6]$$

where P is the first order differential operator and λ the regularization parameter which controls the weight of the lateral constraint minimization $\|Px\|_2$ with respect to the residual norm minimization $\|Ax - b\|_2$.

Several methods allowing the determination of the regularization parameter λ exist; the most recent and reliable are the *L-Curve* (LC) [HAN 93] and *Self-Consistency* (SC) [HON 90].

12.6. Results

The FLIMM technique allows charge profiles to be obtained in 1-D [AGN 05], 2-D [PET 04a] or 3-D [PET 06]. The main advantage of this method is linked with its ability in getting multidimensional charge cartographies, with very good spatial resolutions: 1 µm in depth and 10 µm for lateral resolution.

The following sections present the results obtained by FLIMM for 1-D, 2-D and 3-D charge distributions.

12.6.1. *1-D study of PEN (Polyethylene Naphtalate) subjected to high fields*

The films used for these measurements were supplied by DuPont de Nemours (Luxembourg) (stabilized films with bi-axial orientation). For these 25 µm thick films, the crystallinity rate is about 44%. The samples were metallized with a 30 nm gold layer on which a thin ink layer was deposited in order to increase the optical

absorption of the laser beam. These films were polarised at room temperature for 30 minutes and the applied field was chosen in a range from 12 kV/mm to 300 kV/mm. They were then placed in short circuit conditions for 30 minutes [AGN 05].

The residual field and space charge profiles obtained after 30 minutes of depolarization are presented in Figures 12.3 and 12.4. The charge profiles shown in Figure 12.4 were obtained by measurements made on both sides of the sample. Indeed, the in-depth information given by thermal methods is not sufficient if only one side of the study is considered, and thus, a second measurement is often necessary. This implies a resolution loss around the middle of the sample, and therefore all interpretations are limited close to interfaces. In these zones, an accumulation of homocharges (positive charges at the anode and negative at the cathode) can be noticed, which increase with the field. At low field, the charge density is very weak ($\sim 0.5\, C/m^3$) and can be associated with a dipolar orientation. On the other hand, a massive charge injection appears for fields greater than 225 kV/mm.

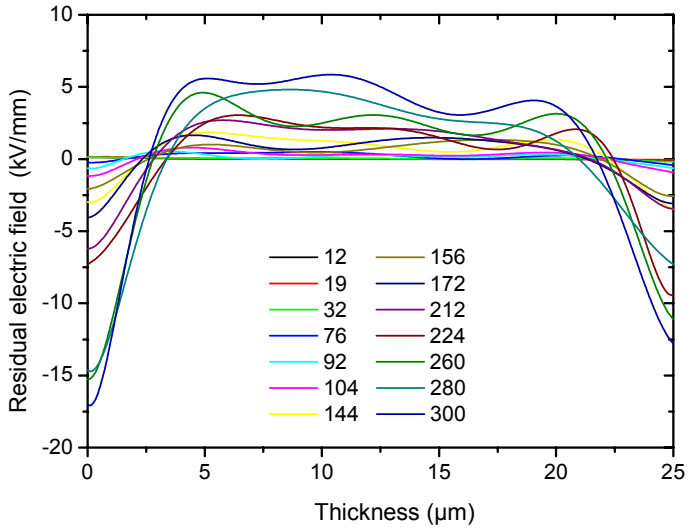

Figure 12.3. *Residual internal fields as a function of the applied voltage*

Close to the anode, the development of a positive homocharge is revealed by the increase of peak charges. It can also be noticed that the level of charges accumulated at the anode is greater than at the cathode.

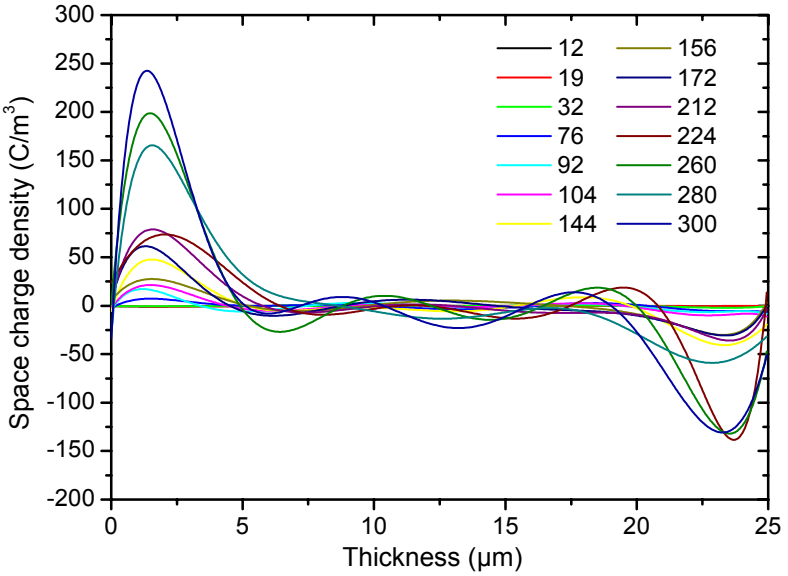

Figure 12.4. *Space charge distribution*

From the distributions in Figure 12.4, the average value of charges located in zones near the interfaces was calculated on a thickness of 5 μm and from each electrode. The values obtained for each curve are presented in Figures 12.5(a) and (b).

Three zones can be distinguished, corresponding to the zones already revealed by Augé *et al.* [AUG 00] using I(V) and electroluminescence measurements.

In the first zone, the charge density is very weak, which means that there is no injection in the range of fields from 12 kV/mm to 75 kV/mm.

Between 75 and 160 kV/mm, a charge injection is produced from the electrodes. Augé *et al.* [AUG 00] showed that in this field range, the current increases in a non-linear way, but there is still no permanent electroluminescence emission. Furthermore, by space charge measurements with the LIPP technique, an injection of homocharges from electrodes was enhanced. For higher fields (160–300 kV/mm), a massive charge injection takes place. This injection is also correlated with a significant increase of the current and electroluminescence with the field. These results are in agreement with others achieved by current and electroluminescence measurements on similar samples.

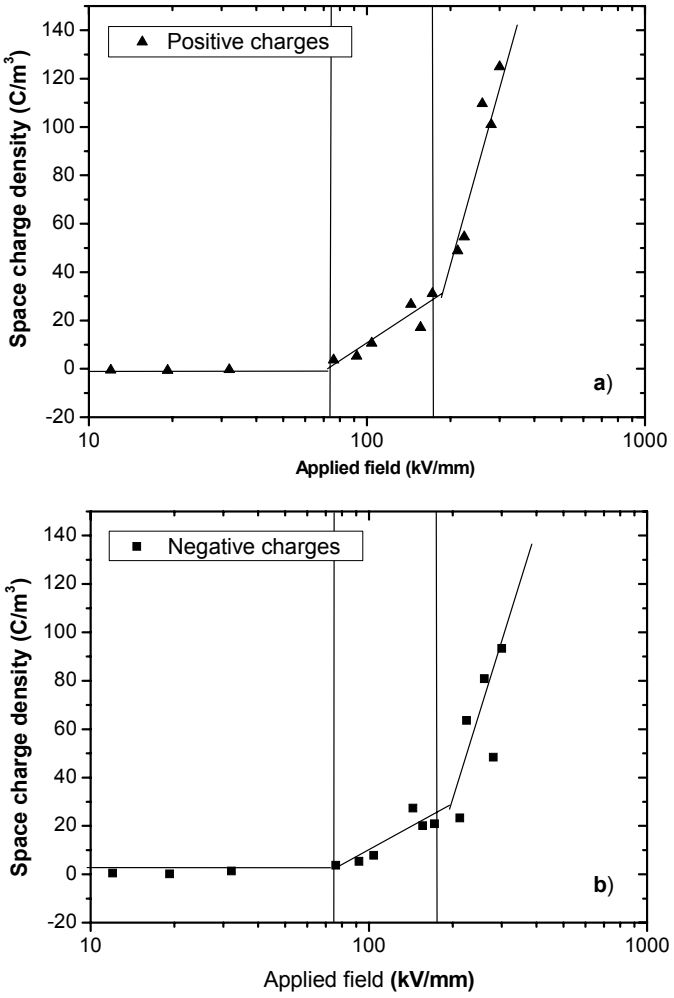

Figure 12.5. *Average space charge values as a function of the applied field: (a) positive charges near the anode; (b) negative charges near the cathode*

12.6.2. *2-D charge distribution*

The FLIMM method was also used for the study of space charges induced by ultraviolet (UV) irradiation, as a complement of electroluminescence measurements [PET 04b].

In our research, electroluminescence measurements were carried out on thin PEN films. It was noted that the emission of the electroluminescence was weaker on the irradiated zones. This phenomenon was associated with the apparition of space charges within the irradiated zones. To confirm (or invalidate) this hypothesis, space charge measurements were undertaken using FLIMM.

For this purpose, thin Poly(ethylene 2.6-naphthalene) films (PEN, DuPont de Nemours) were used. Space charge measurements were made on 25 µm thick films, and on 50 µm ones for electroluminescence studies.

The samples' ageing was induced by UV rays from a 30W insulating system used for printed circuits production. The sample subjected to UV presented a special configuration of space charge measurements, showed in Figure 12.6. During irradiation, the sample was protected by a mask, and only three zones were irradiated, for different durations of, respectively, 12, 24 and 48 hours. The irradiated zones are here represented by circles of 1 mm diameter.

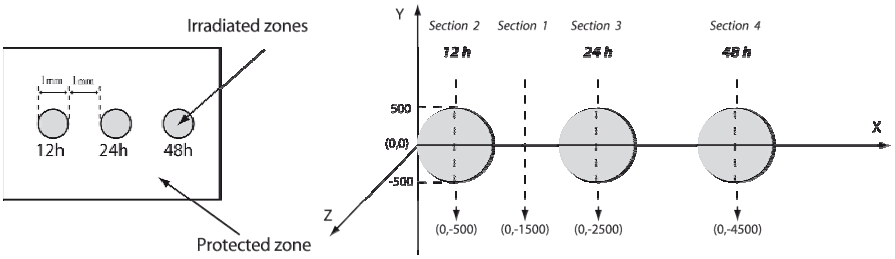

Figure 12.6. *Configuration of the sample for space charge measurements*

After the irradiation, a semi-transparent gold layer (50 nm) was sputtered on both sides of the sample. Finally, a thin carbon layer was sputtered on the irradiated zones in order to facilitate sample positioning and analysis.

The space charge measurements were made according to the X and Y axes, with a 50 µm step (Figure 12.6). The results obtained in both directions being similar, only results according to the Y axis are presented. The Z axis is the direction of the sample thickness.

Section 1 of Figure 12.7 presents the cartography of a non-irradiated zone; Sections 2, 3 and 4 show those of irradiated zones for 12, 24 and 48 hours. For each section, 22 measurement points were necessary. The acquisition of a measurement point was made in a frequency range of 100 Hz to 10 kHz, requiring 6 minutes for the total recording.

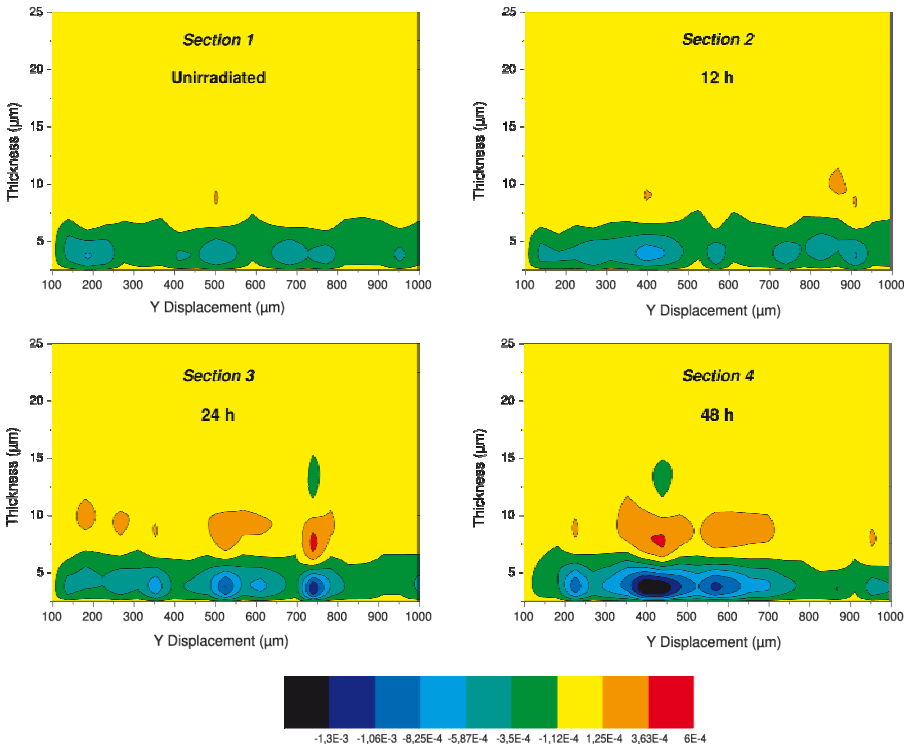

Figure 12.7. *Space charge cartographies for different irradiation durations*

Figure 12.7, Section 1, gives the charge distribution relative to Section 1 (the non-irradiated zone) and it will be considered as a reference. By visual analysis, it can be seen that there is not a great difference between Sections 1 and 2. This expresses the fact that the material is not affected by the irradiation for weak exposure durations (<12h). On the other hand, the charge level increases with exposure time. For a 24-hour irradiation, negative charges appear in a zone near the surface, in a non-homogenous way. For 48 hours, the charge level becomes important compared with the reference profile level, and the accumulation zone becomes wider.

Another important observation concerns the depth of the charge accumulation zone. This one, situated near the surface of the sample, is present in all sections studied and its spreading depends on exposure time. This result was expected, considering that the photo-oxidation induced by UV irradiation is a surface phenomenon [SCH 97].

Effects of UV on the PEN were also studied by IR micro-profilometry [SCH 97]. The authors showed that the photo-oxidation of the material does not exceed 10μm. This result is in agreement with that obtained by FLIMM. Indeed, the cartographies show that the space charges are confined in a zone near the surface, at about 7 μm depth.

Furthermore, the degraded zone at the surface of the sample becomes very absorbant, causing a yellowing of the material, thus constituting a protection screen for the rest of the material. This surface phenomenon was also revealed by photoluminescence measurements [MAR 01] taken in our laboratory.

The space charge measurements showed that during the UV-irradiation, an accumulation of charges takes place at the surface of the material. This phenomenon is probably at the basis of the material's electroluminescence level reduction. Thus, EL and FLIMM appear to be complementary techniques for the study of ageing phenomena induced by UV. New measurements were planned using both techniques in order to determine the detection limits in a quantitative manner, particularly concerning the minimal irradiation surface, the irradiation intensity or durations of exposure.

12.6.3. *3-D charge distributions*

12.6.3.1. *Sample preparation*

For three-dimensional cartographies [PET 06], the following conditions must be fulfilled:

– the material under study must trap charges for a long period of time;

– the zones where space charges are accumulated must be easy to identify.

The first condition is important because the execution of the cartography requires the recording of several measurement points according to surface scanning in X and Y directions. The total acquisition of data can last several days, hence the importance of a material possessing the ability to store charges for a long time. To that purpose, the choice was made of Teflon (PTFE) polymer, as it is well known for its charge trapping properties.

The exact knowledge of the zones likely to contain space charges is obtained by the prior pasting of a microscope grid on the sample. The grid allows a selective implantation of electrons according to its geometry. By knowing the physical characteristics of the grid used with high accuracy (i.e. the dimensions of the squares), the zones in which charges were implanted can be precisely determined.

The samples used for this study are thin (50 µm thick) PTFE films, metallized on both sides with a 30 nm gold layer. Microscope grids with different geometries were stuck on the samples, either with silver paint, or with cyanolite. The samples were irradiated by a scanning electron microscope (SEM, JEOL JSM- 6060LV) and then a very thin layer of carbon (~20 nm) was evaporated on the whole sample. This allows a print of the grid to be kept once the mask is removed.

12.6.3.2. *3-D cartographies*

Six measurement points organized according to X and Y axes, and 50 µm spaced, are depicted in Figure 12.8. The Z axis still represents the direction of the sample thickness.

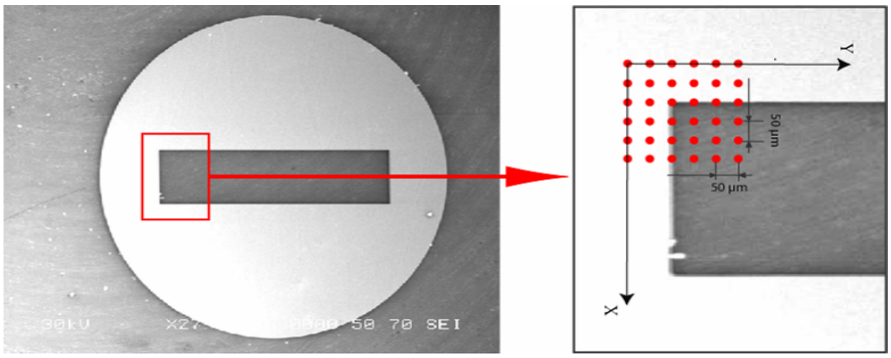

Figure 12.8. *Visualization of the analysis zone*

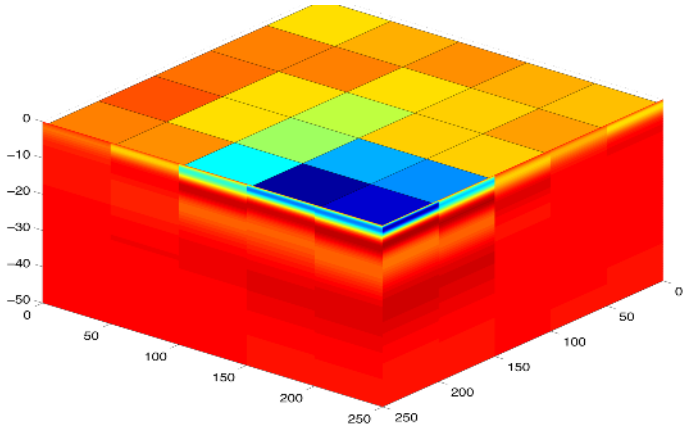

Figure 12.9. *3D Visualization of the charge distribution*

The 3-D charge representation obtained is shown in Figure 12.9.

First of all, electrons seem to remain confined in a zone near the sample surface. However, this zone is slightly smaller than the irradiated zone. This could be explained by edge effects due to a non-homogeneous implantation of electrons in the vicinity of the grid edges. The 3-D cartography is very coherent with the configuration of the sample; nevertheless, the spatial resolution can be improved.

An interesting study was to test and reach the limits of FLIMM, in terms of spatial resolution as well as sensitivity, with respect to the charge evolution with time. For this purpose, similar samples elaborated and irradiated in the same way as previous ones were studied. The grid used this time had vertical bars of different width. The chosen zone for this new study is presented in Figure 12.10. The measurement points are 10 µm spaced in the X direction, and 50 µm spaced according to the Y axis; 44 measurements per line were used for a total measurement duration of 2 days.

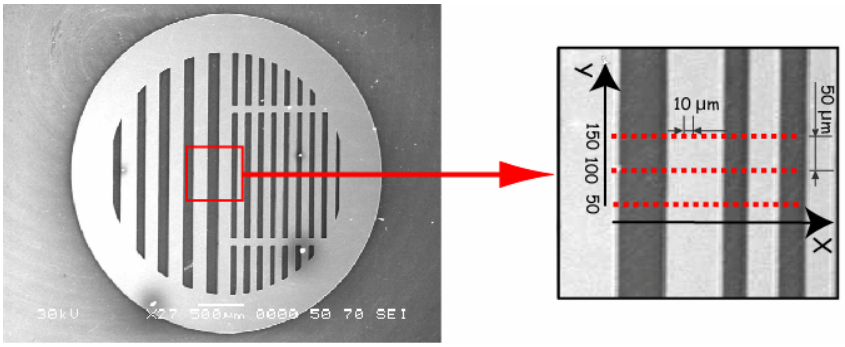

Figure 12.10. *Analysis zone*

Figure 12.11 gives a multi-dimensional representation of charges which have been implanted. It should be noted that negative charges were efficiently implanted in the non-protected zones.

It is also important to note that the charge distributions detected in FLIMM correspond exactly to the implantation conditions and according to the grid geometry. The total charge penetration depth is about 5 µm, with a peak around 2 µm.

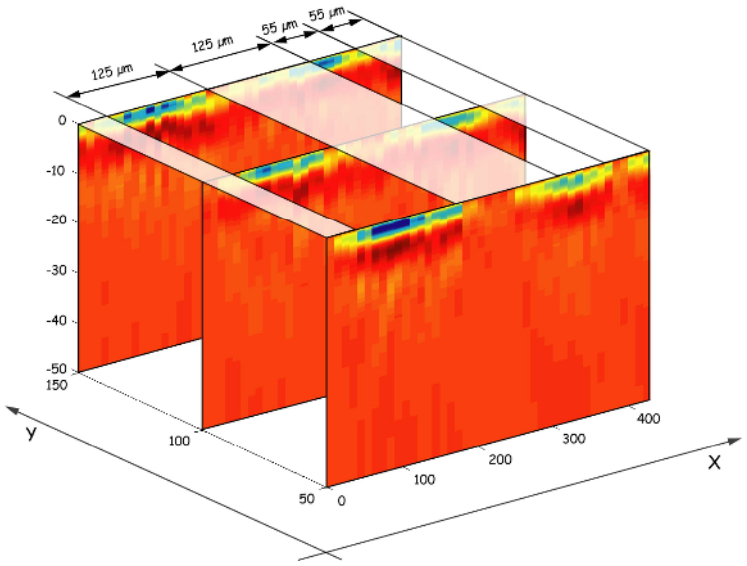

Figure 12.11. *Representation of the implanted charge with the visualization of bars*

12.7. Conclusion

In this chapter, the FLIMM method was presented from both a theoretical point of view and with experimental results. Some of its specificities for the execution of multidimensional representations of space charges in solid insulators have been shown. The results obtained show that FLIMM can be used as a diagnosis tool with a lateral spatial resolution of about 10 µm, that is to say 1,000 times lower than other more traditional methods (PEA, thermal wave, etc.).

This resolution could be improved by decreasing the spot size as well as increasing the upper modulation frequency, which will require more complex developments (which are under way).

12.8. Bibliography

[AND 77] ANDREWS H. C., HUNT B. R., *Digital Image Restoration*, Prentice-Hall, Englewood Cliffs, 1977.

[AGN 05] AGNEL S., NOTINGHER JR P., CASTELLON J., TOUREILLE A., FRANCESCHI J.L., LAURENT C., MARTY-DESSUS D., MARY D., PETRE A., TEYSSEDRE G., "Comportement diélectrique du polyéthylène téréphthalate (PET). Mesures de charges d'espace", *Revue Internationale de Génie Electrique*, vol. 8, no. 2, p. 205–220, 2005.

[AUG 00] AUGÉ J. L., TEYSSÈDRE G LAURENT C., DITCHI T., HOLÉ S., "Combined electroluminescence and charge profile measurements in poly(ethylene-2.6-naphthtalate) under a DC field", *J. Phys. D: Appl. Phys*, vol. 33, p. 3129–33138, 2000.

[FRA 97] FRANCESCHI J.L., HAAS V., "Laser thermoacoustic modulation for space charge measurement", *Appl. Phys. Letts*., vol. 70, no. 17, p. 2236–2237, 1997.

[FRA 00] FRANCESCHI J.L., MARTY-DESSUS D., BIELLMANN C., BERQUEZ L., MOUSSEIGNE M., "Profils de charges d'espace dans les isolants polymères minces par une méthode d'excitation thermique avec laser focalisé", *Congrès SFE 2000*, Montpellier, 2000.

[FRA 01] FRANCESCHI J. L., BIELLMANN C., BERQUEZ L., MARTY-DESSUS D., "Virtual Space Charge Model for a frequency-based characterization of insulators", *Jpn. Journal of Applied Physics*, vol. 40, p. 880–890, 2001.

[HAS 97] HAAS V., MOUSSEIGNE M., FRANCESCHI J.L., *J. Electrostatics*, vol. 40–41, p. 307–312, 1999.

[HAN 93] HANSEN P.C., O'LEARY D.P, "The use of the L-curve in the regularization of discrete ill-posed problems", *SIAM J. Sci. Comput*., vol. 14, no. 6, p. 1487–1503, 1993.

[HAN 94] HANSEN P. C., "Regularization Tools: A Matlab package for analysis and solution of discrete ill-posed problems", *Num. Algorithms*, vol. 6, p. 1–35, 1994.

[HAN 96] HANSEN P. C., MOSEGAARD K. "Piecewise polynomial solutions without *a priori* break points", *Num. Lin. Algebra with Appl*., vol. 3, no. 6, p. 513–524, 1996.

[HON 90] HONERKAMP J., WEESE J., "Tikhonovs regularization method for ill-posed problems", *Continuum Mech. Thermodyn*, vol. 2, p. 17–30, 1990.

[LAN 81] LANG S. B., DAS-GUPTA D. K., "A technique for determining the polarization distribution in thin polymer electrets using periodic heating", *Ferroelectrics*, vol. 39, p.1249–1252, 1981.

[LAN 91] LANG S. B., "Laser intensity modulation method (LIMM): Experimental techniques, theory and solution of the integral equation", *Ferroelectrics*, vol. 118, p. 343–361, 1991.

[LAN 98] LANG S. B., "An analysis of the integral equation of the surface Laser Intensity Modulation Method using the constrained regularization method", *IEEE. Trans. on Dielec. Electr. Insul.*, vol. 5, no. 1, p. 70–76, 1998.

[MOP 82] MOPSIK F.I., DEREGGI A.S., *J.Appl. Phys.* vol. 53, 4333–4339, 1982.

[PET 04a] PETRE A., Optimisation de la méthode FLIMM pour la caractérisation en volume des charges d'espace dans les isolants polymères minces, Doctoral thesis, Paul Sabatier University, Toulouse, December 2004.

[PET 04b] PETRE A., MARY D., MARTY-DESSUS D., "Study of PEN ageing under UV irradiation by electroluminescence and space charge measurements", *J. Optoel. and Adv. Mat*, vol. 6, no. 3, p. 1049–1054, 2004.

[PET 04a] PETRE A., MARTY-DESSUS D., BERQUEZ L., FRANCESCHI J.L., "A Comparison of Different Mathematical Treatments for Solving the Inverse Problem in Focused Laser Intensity Modulation Method", *Jpn. Journal of Applied Physics*, vol. 43, no. 5A, p. 2572–2579, 2004.

[PET 06] PETRE A., MARTY-DESSUS D., BERQUEZ L., FRANCESCHI J.L., "Space Charge Cartography by FLIMM on Thin PTFE Films Irradiated by Scanning Electron Microscope", *J. Electrostatics*, vol. 64, nos. 7–9, p. 492–497, July 2006.

[PLO 92] PLOSS B., EMMERICH R., BAUER S., "Thermal wave probing of pyroelectric distributions in the surface regions of ferroelectric materials – A new method for the analysis", *J. Appl. Phys*., vol. 72, p. 5363–5370, 1992.

[SCH 97] SCHEIRS J., GARDETTE, J.-L., "Photo-oxidation and photolysis of poly(ethylene naphthalate)", *Polym. Degr. Stab*., vol. 56, p. 339–350, 1997.

[SKI 02] SKIPA O., NALBACH M., SACHSE F. B., DOSSEL O., "Comparison of regularization techniques for the reconstruction of transmembrane potentials in the heart", *Biomedizinische Technik*, vol. 47, p. 246–248, 2002.

[TAK 99] TAKADA T., "Acoustic and Optical Methods for Measuring Charge Distribution in Dielectrics", *Proc. IEEE CEIDP*, p. 1–14, Austin, USA, 1999.

[TIK 77] TIKHONOV A.N., ARSENIN V.Y., *Solution of Ill-posed Problems,* Wiley, New York, 1977.